Background Motivation

RCNP核理I論文紹介:
2009.03.24 by A. Tamii

RCNP-E314

Search for Direct Evidence of Tensor Interaction:
High Momentum Component in Nuclei

I. Tanihata, H. J. Ong, and collaborators

Measurement of (*p*,*d*) and (*p*,*dp*) reactions on ^{12}C and ^{16}O targets using proton beams at 200, 300, and 392 MeV in search of direct evidence of tensor interaction in high-momentum component in nuclei.

"Tensor Correlation"

"High-Momentum Component"

"Short Range Correlation"

Tensor力 $S_{12} \equiv 3\frac{(\boldsymbol{\sigma}_1 \cdot \mathbf{r})(\boldsymbol{\sigma}_2 \cdot \mathbf{r})}{r^2} - (\boldsymbol{\sigma}_1 \cdot \boldsymbol{\sigma}_2)$

$$< \Phi_f \,|\, \sum_m c_m S_{..} S_{..} Y_2^m \,|\, \Phi_i >$$

N-*N*ペアの波動関数
(スピン1)

$$\mathbf{S} = \mathbf{S}_1 + \mathbf{S}_2 = \frac{1}{2}\hbar(\boldsymbol{\sigma}_1 + \boldsymbol{\sigma}_2)$$

$$S_{12} = \frac{2}{\hbar^2}\left[\frac{(\mathbf{S}\cdot\mathbf{r})^2}{r^2} - \frac{1}{3}(\mathbf{S}\cdot\mathbf{S})\right]$$

$$= \left(\frac{24}{5}\pi\right)^{1/2}\left[S_-^2 Y_2^2 - (S_- S_z + S_z S_-)Y_2^1 + \sqrt{\frac{2}{3}}(3S_z^2 - \mathbf{S}^2)Y_2^0 + (S_+ S_z + S_x S_+)Y_2^{-1} + S_+^2 Y_2^{-2}\right]$$

今回紹介する論文:

Probing Cold Dense Nucleon Matter
R. Subedi, *et al*., Science 320, 1476 (2008)

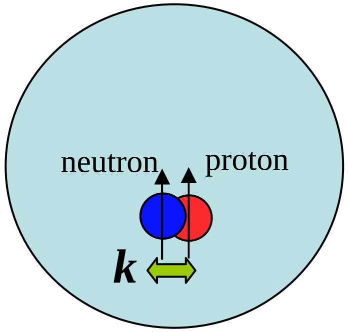

n–*p*ペアの核内での短距離相関
(Short Range Correlation)

(今回対象では)スピン1に組んでおり、相対的に高運動量をもっているがペアの重心はほぼ静止している。

核子間テンソル力が原因と考えられる。

p–pやn–nの相関に比べて圧倒的に大きい(20倍)。

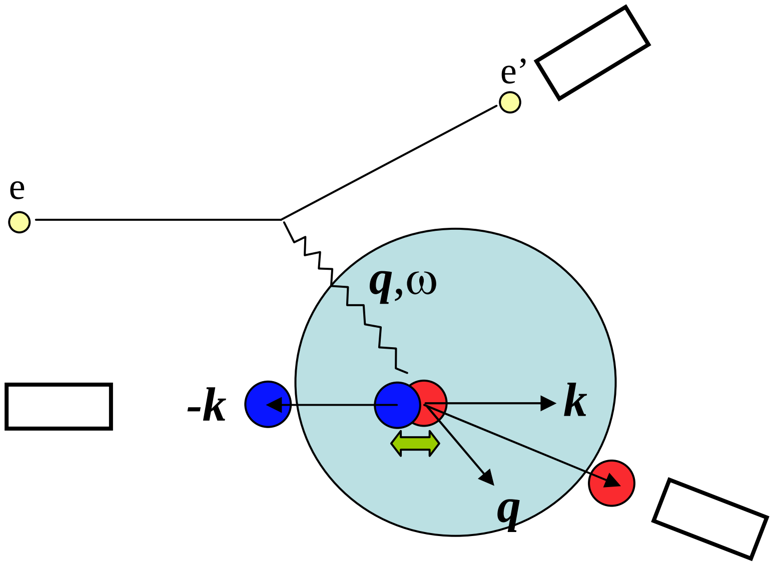

陽子がたたき出された時に、逆方向に中性子が放出される確率を測定

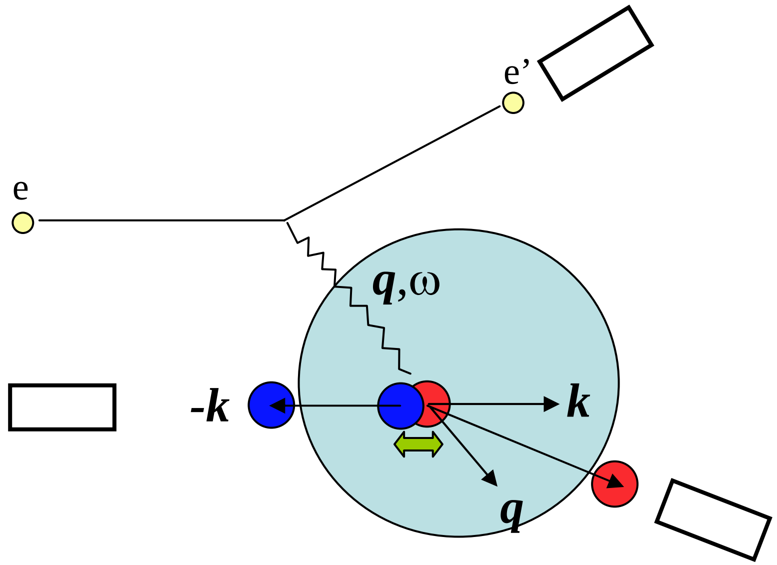

イベント量(散乱断面積)
の違いを見るのが1つ
のポイント

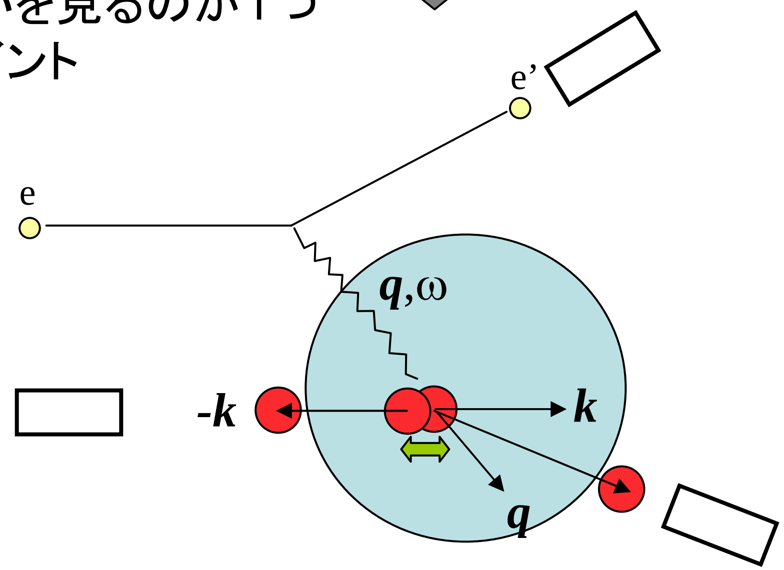

RCNP-E314

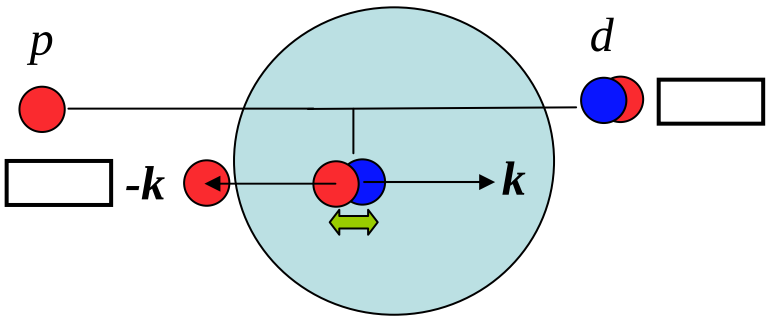

· 強い相互作用で反応（散乱断面積が大きい）

· (p,d)反応で、k:大 成分を選択的にピックアップ
(p,p’n)に比べて多段階散乱などの寄与を防げる、検出効率も高い

· 反応メカニズムが複雑

· 反応が原子核の表面で起きやすい？

· n-p pair の寄与を見るために n 検出を要しない。

Much more sophisticated だが
明確な結果を引き出せるか？

(e,e’pn)

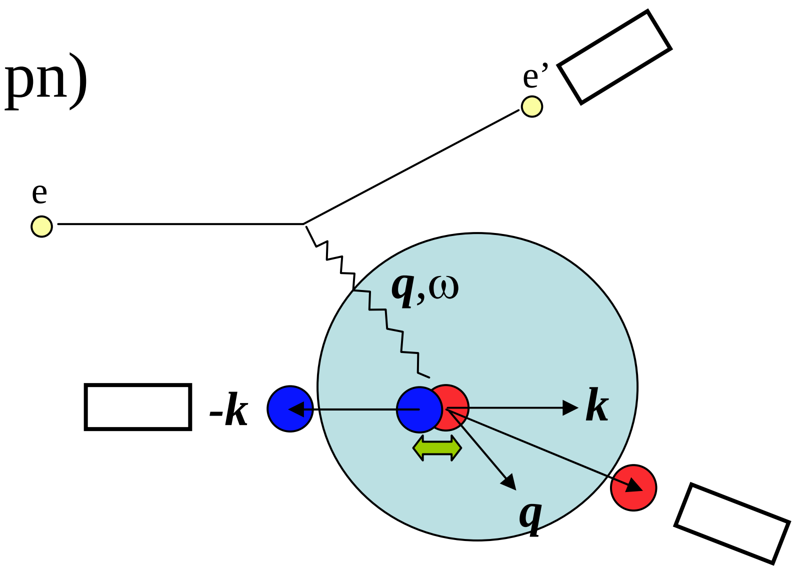

·電磁相互作用で反応（散乱断面積が小さい）

·反応メカニズムに曖昧性がない

·三重同時測定が必要

· n-p pair の寄与を見るために n 検出を要する。

Brute-Force だが Robust?
統計的につらい！

RCNP-E314 proposal

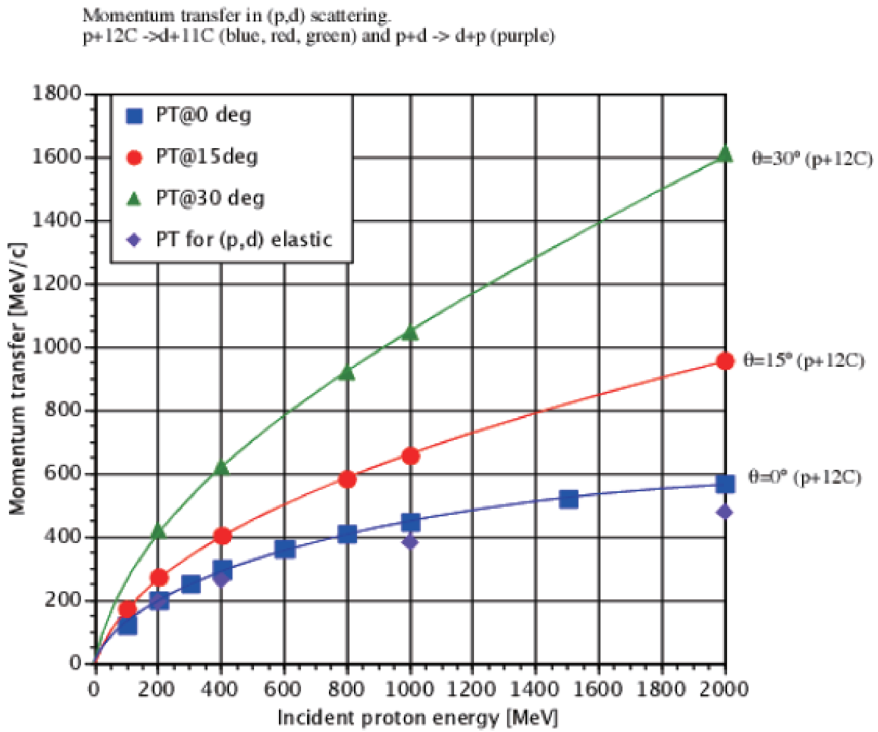

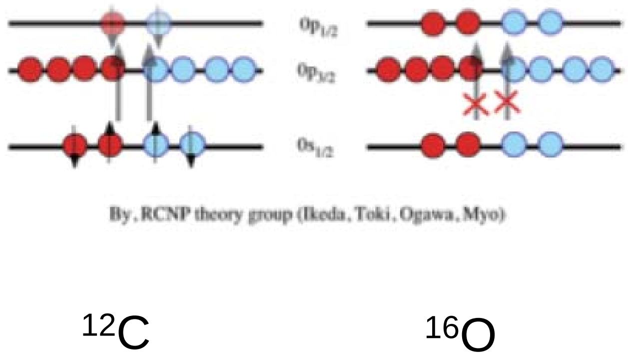

[1] L. Lapikas, Nucl. Phys. A. **553**, 207 (1993)

Quasi-free 電子散乱
(e,e’p)

at NIKHEF

Spectroscopic Factor

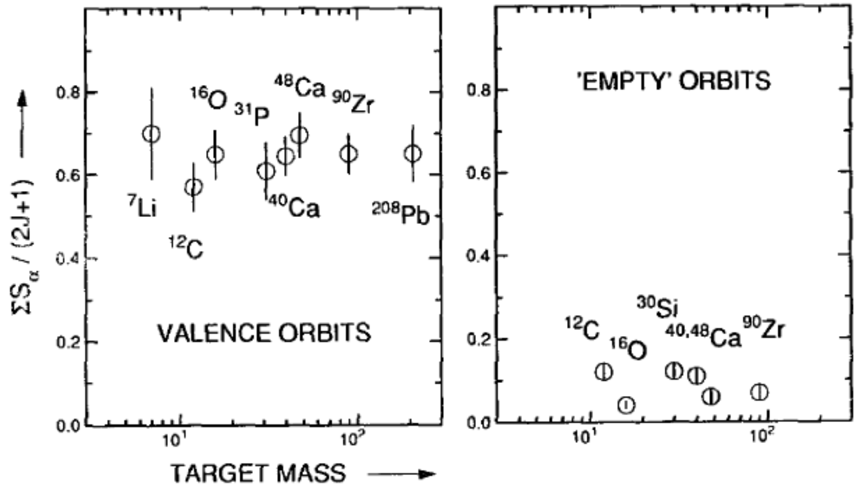

Fig. 9. Quasi-particle strength $\Sigma S_\alpha/(2j+1)$ for valence orbitals (left panel) and for states just above the Fermi edge (right panel), observed in the reaction (e,e'p) as a function of the mass of the target nucleus. All strengths were integrated to an excitation energy of about 20 MeV.

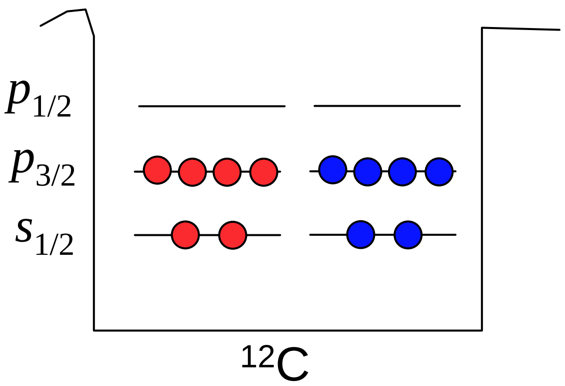

shell model的描像
“Independent Particle Motion”

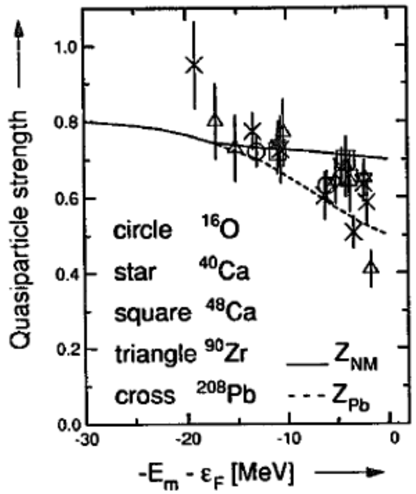

Fig. 11. Summed spectroscopic strength observed for proton knockout from various orbitals in the closed-shell nuclei ^{16}O [41], ^{40}Ca [33,38], ^{48}Ca [33], ^{90}Zr [32] and ^{208}Pb [19,48] as a function of the mean excitation energy of the orbital relative to the Fermi edge. The dashed curve represents the quasi-particle strength calculated for nuclear matter, the solid curve is derived from the nuclear matter curve by including surface effects calculated for ^{208}Pb [4].

shell model描像の独立粒子軌道には、60-70%ほどの核子しか存在しない！

2p1hや1p2hの2nd-order self-energy の効果
coupling to collective excitations
c.m. spurious motion の補正...

Long Range Correlations (LRC) ... several fm ... [3]

S-factor 減少を半分も説明できない

Short Range Correlations (SRC) ... ≦ 1 fm ... [4-12]

NN pair with
large relative momentum
small center of mass momentum
scalar and tensor *NN* interaction

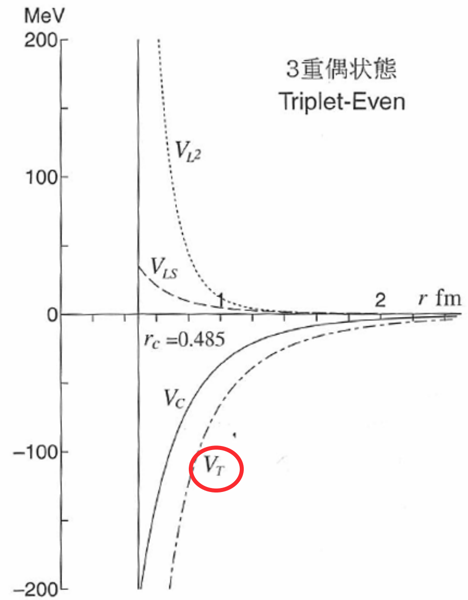

図 2.3 HJ ポテンシャル (^{3}E)

高運動量の陽子がノックアウトされた場合、その運動量は、1つの反跳核子によってバランスされる。

逆もまた真なり？必ずしもそうではないがかなり有力。

高運動量核子は、主にSRC pairing によって生じる。(理論)

n-p pair と p-p pair の差を見るのが鍵！
テンソル力による相関がかなり強く示唆される。

JLab, Hall-A

Beam: electron, 4.627 GeV, 5 and 40 μA

Target: C graphite sheet, 0.25 mm^t (~50 mg/cm^2)

Kinematical Condition: q=1.65 GeV/c , ω= 865 MeV

Missing Momentum of (e,e'p) : 300-600 MeV/c

(e,e'p) trigger rate: 0.2 Hz

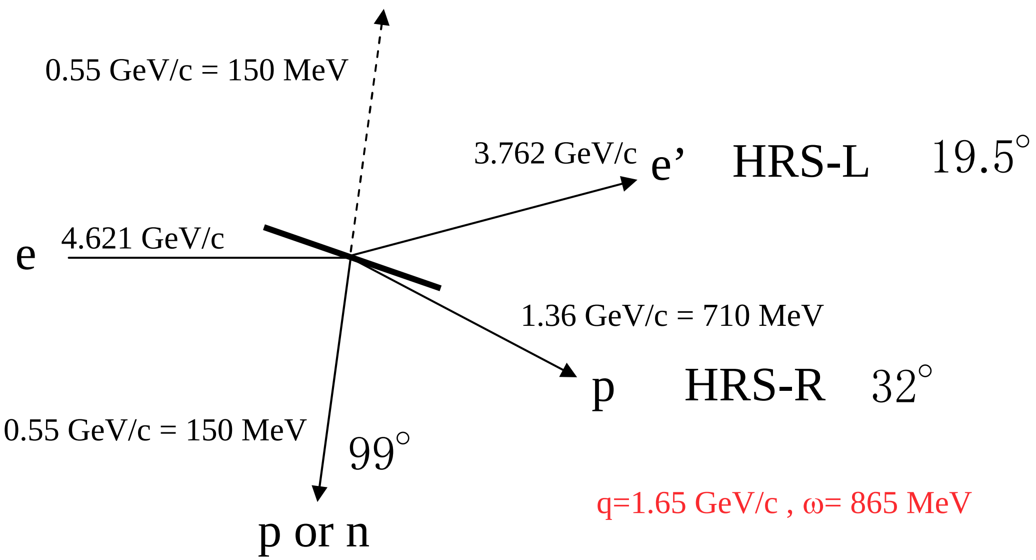

BBS or Neutron Array

[15] J. Alcorn et al., NIMA 522, 294 (2004)

JLab, Hall-A

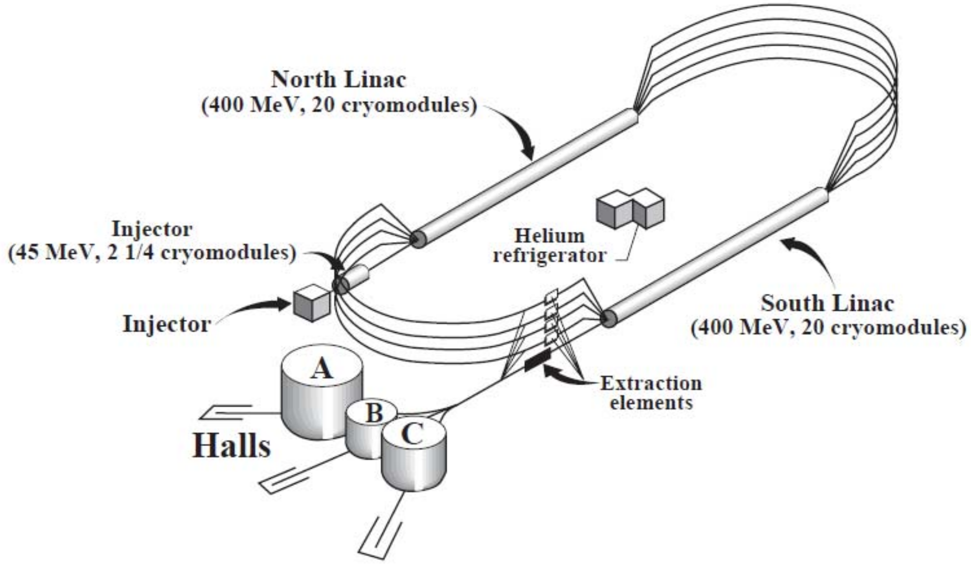

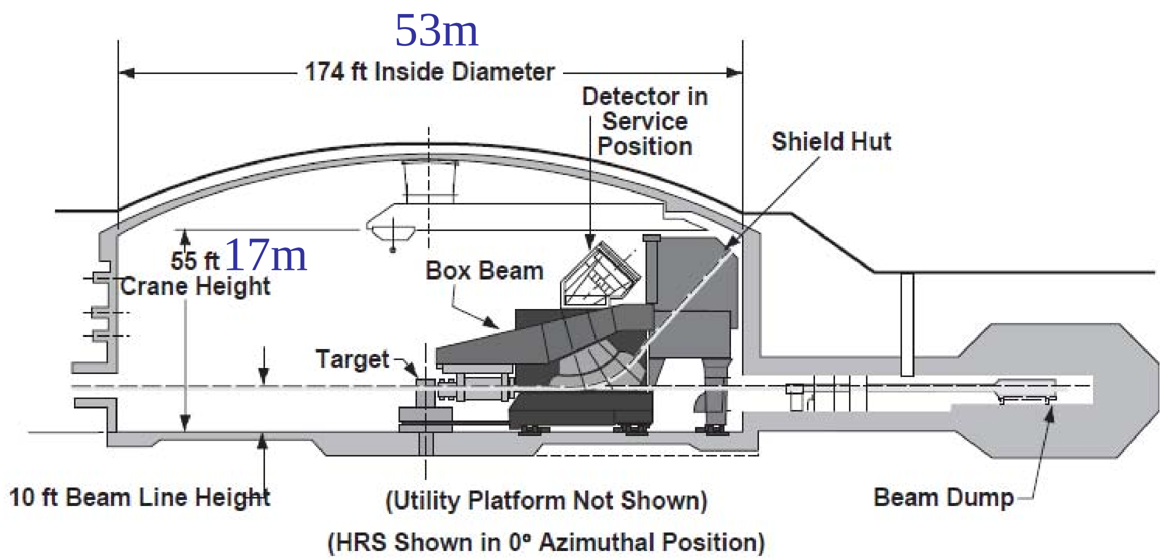

[15] J. Alcorn et al., NIMA 522, 294 (2004)

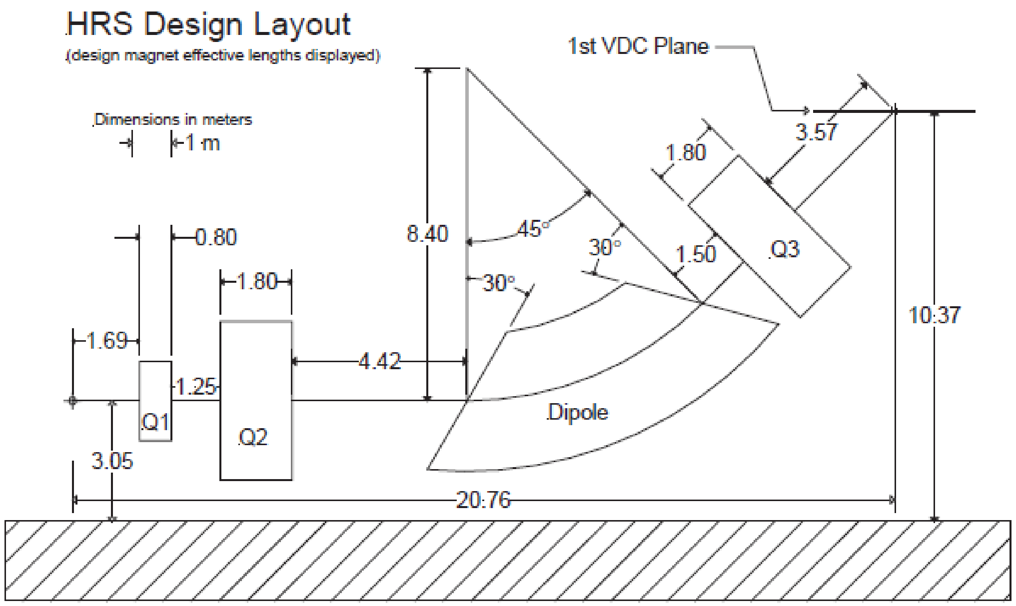

Table 1
Main design characteristics of the Hall A high resolution spectrometers; the resolution values are for the FWHM

Configuration	QQD_nQ vertical bend
Bending angle	45°
Optical length	23.4 m
Momentum range	0.3–4.0 GeV/c
Momentum acceptance	$-4.5\% < \delta p/p < +4.5\%$
Momentum resolution	1×10^{-4}
Dispersion at the focus (D)	12.4 m
Radial linear magnification (M)	−2.5
D/M	5.0
Angular range	
HRS-L	12.5–150°
HRS-R	12.5–130°
Angular acceptance	
Horizontal	±30 mrad
Vertical	±60 mrad
Angular resolution	
Horizontal	0.5 mrad
Vertical	1.0 mrad
Solid angle at $\delta p/p = 0$, $y_0 = 0$	6 msr
Transverse length acceptance	±5 cm
Transverse position resolution	1 mm

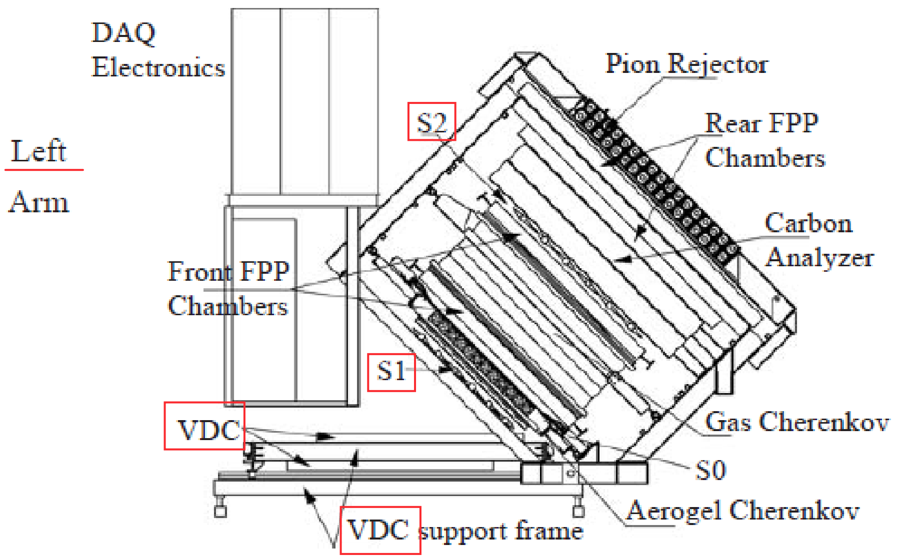

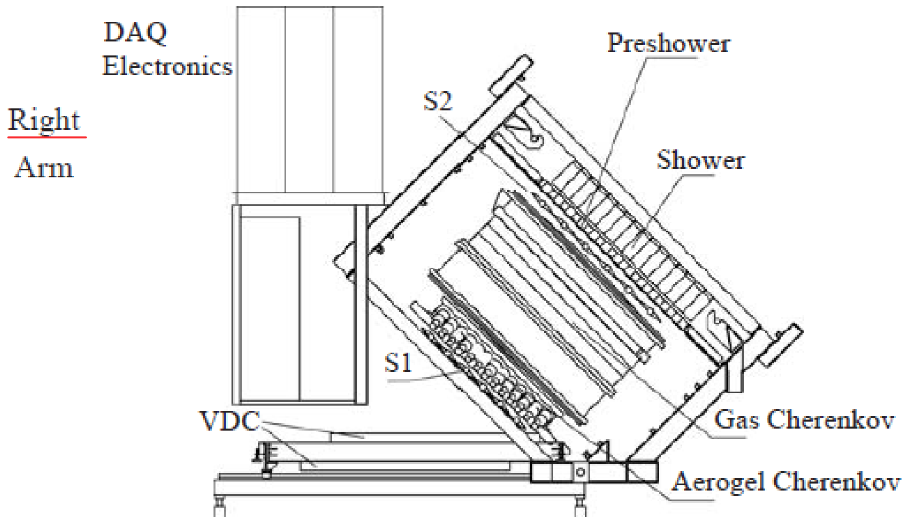

S1,S2: plastic scintillators

BBS: [16] Supplement

96msr, 0.25-0.9 GeV/c, three planes of plastic scintillators

$\delta p/p = 2.5\%$ (from $\delta t = 0.5$ns) at 0.93T

Neutran Array:

88 plastic scintillators at a distance of 6m

$1 \times 3 \times 0.4\ m^3$, lead block of 50mm^t + 20mm^t plastic (c.p. veto)

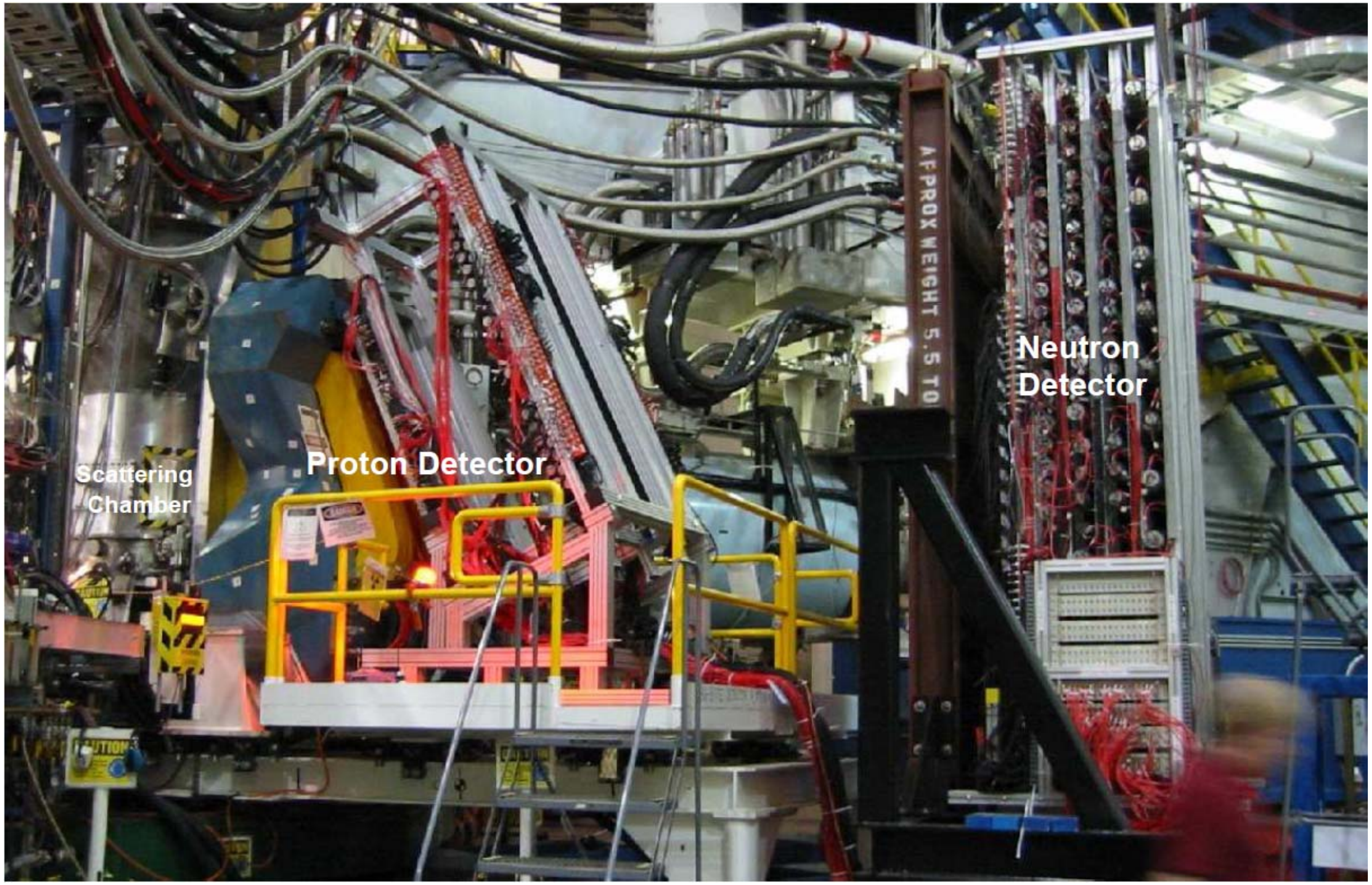

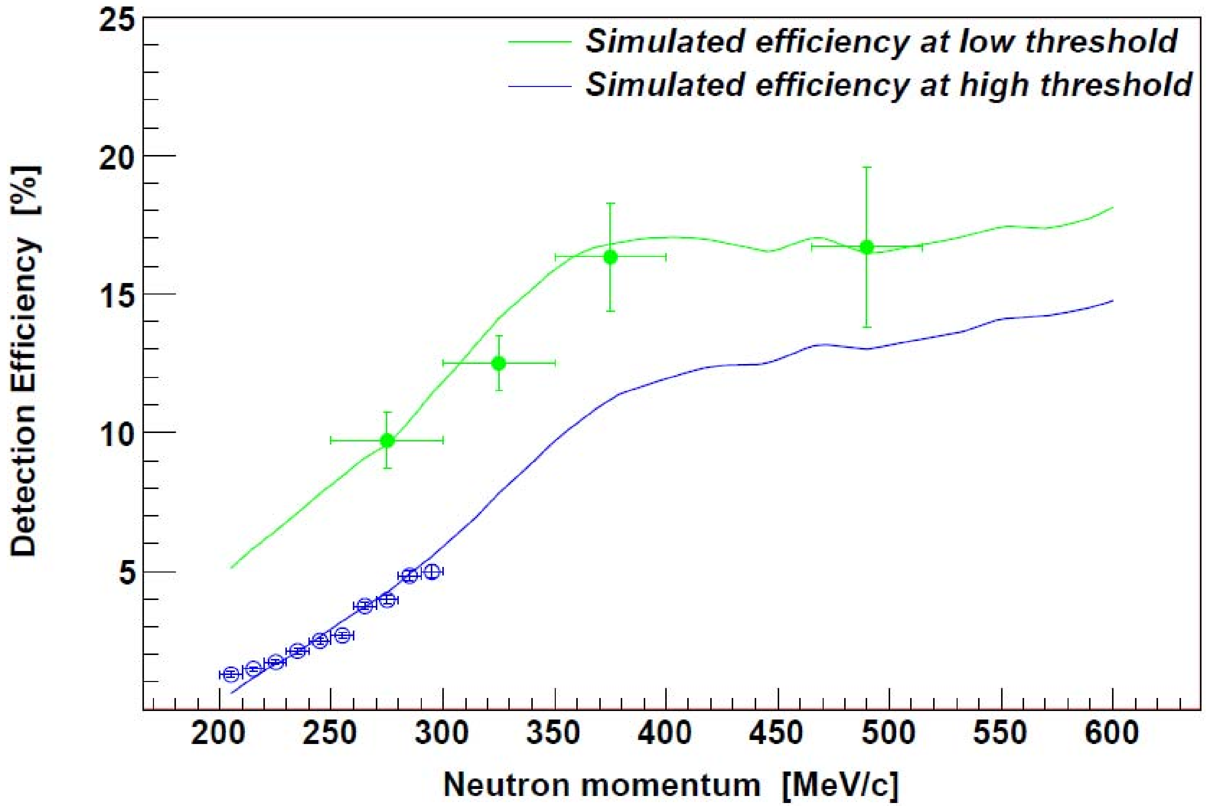

Figure S2: Shown is the neutron detection efficiency versus neutron momentum. The data are from the overdetermined quasi-elastic $^2\mathrm{H}(e, e'p)n$ reaction, which was used to make an effective neutron beam while the curves are from a simulation. The green curve is for a 4.627 GeV beam and a low detection threshold, while the blue curve is for a 2.345 GeV beam with a high detection threshold.

[12] Shneor et al., PRL99,072501(2007)

$p_{1/2}$ proton knock-out: ^{11}B(g.s.)

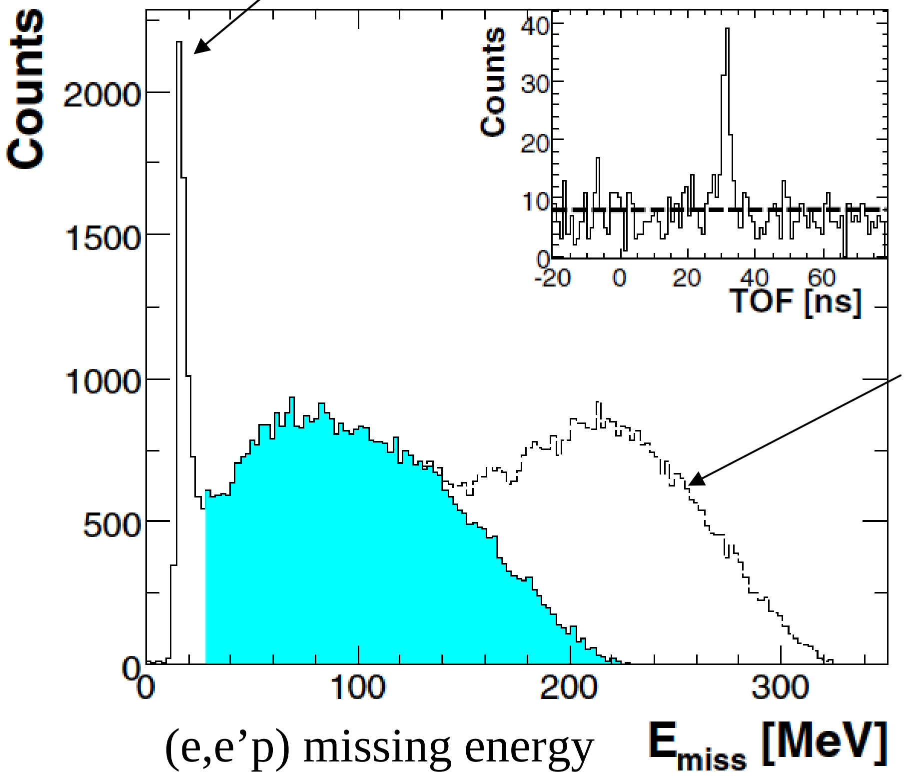

(e,e'p) missing energy

FIG. 2 (color online). The measured $^{12}C(e, e'p)$ missing-energy spectrum for $p_{miss} \sim 0.31$ GeV/c. The peak at 16 MeV is due to removal of p-shell protons leaving the ^{11}B in its ground state. The shaded region contains events with residual excited bound or continuum states. The dashed line contains events in which the Δ was excited. Inserted is the TOF spectrum for protons detected in BigBite in coincidence with the $^{12}C(e, e'p)$ reaction. The random background is shown as a dashed line.

Δ-Excitation の寄与:
missing momentum の方向を前方<~80° に限ることで落とすことができる。

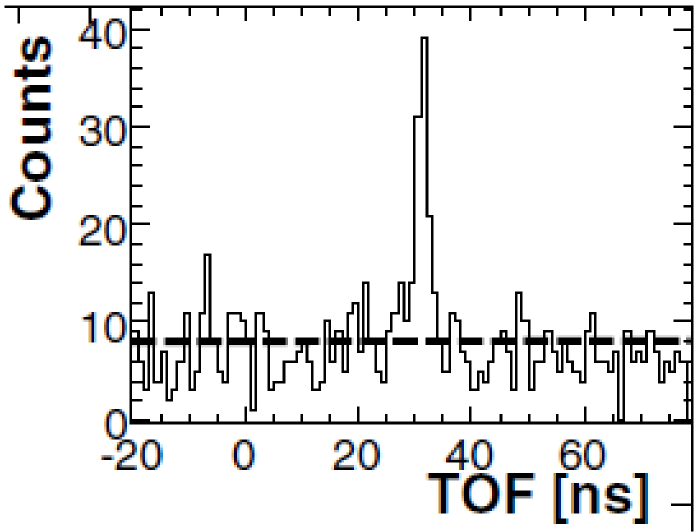

(e,e'pp) TOF (by BBS)
(~100 events?)

[12] Shneor et al., PRL99,072501(2007)

pair の c.m.　momentum は、Gaussian 幅0.136±0.020 GeV/c (by Fitting to the data)
6つの運動学的条件で consistent

from (p,ppn)　... 幅0.143±0.017 GeV/c [9]
Theory　　　　... 0.139 GeV/c　[12[20]]

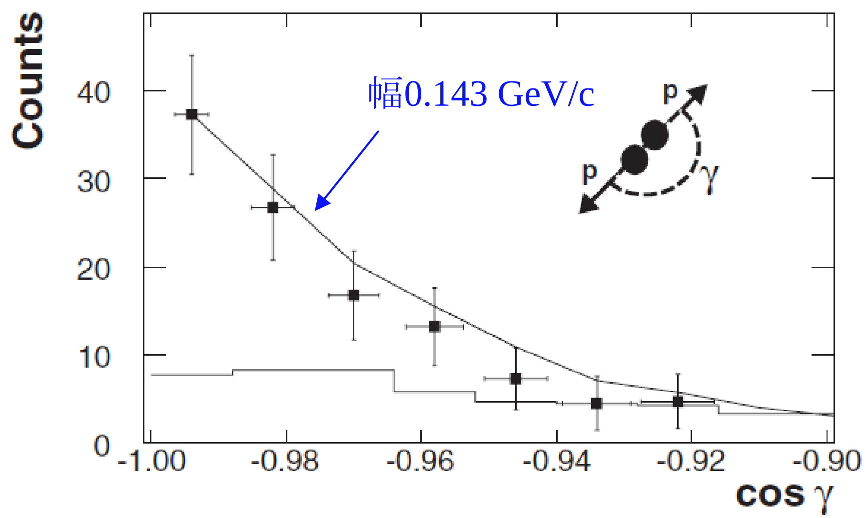

FIG. 3. The distribution of the cosine of the opening angle between the $\vec{p}_{\rm miss}$ and $\vec{p}_{\rm rec}$ for the $p_{\rm miss} = 0.55$ GeV/c kinematics. The histogram shows the distribution of random events. The curve is a simulation of the scattering off a moving pair with a width of 0.136 GeV/c for the pair c.m. momentum.

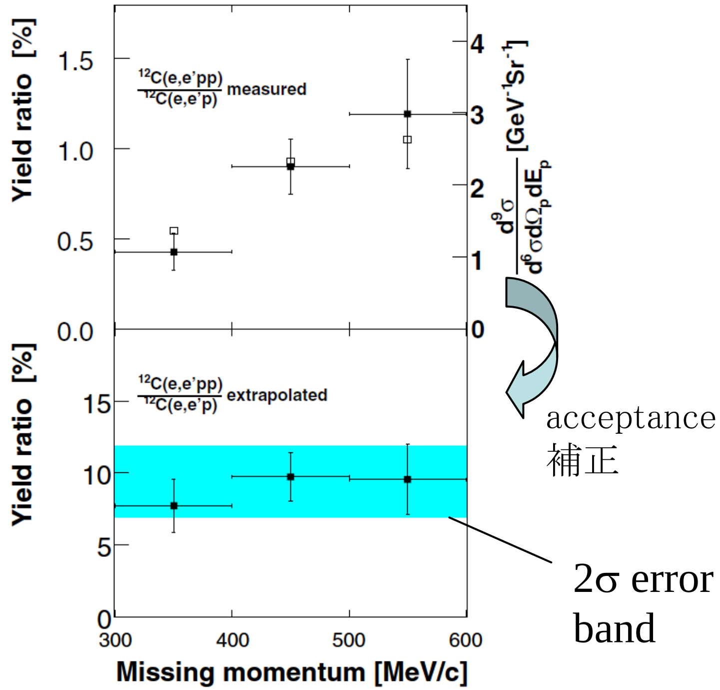

9.5±2%のイベントが、back-to-back の p　を伴う

(0.3<$p_{\rm miss}$<0.6 GeV/c)

Results:

$$\frac{^{12}\mathrm{C}(e,e'pp)}{^{12}\mathrm{C}(e,e'p)} = 9.5 \pm 2\%$$

$$\frac{^{12}\mathrm{C}(e,e'pn)}{^{12}\mathrm{C}(e,e'p)} = 96 \pm 22\%$$

for p-momentum of >300 MeV/c

(~20 events?)

c.f.

$$\frac{^{12}\mathrm{C}(p,ppn)}{^{12}\mathrm{C}(p,pp)} = 92 \pm 18\%$$

for p-momentum of >275 MeV/c [11]

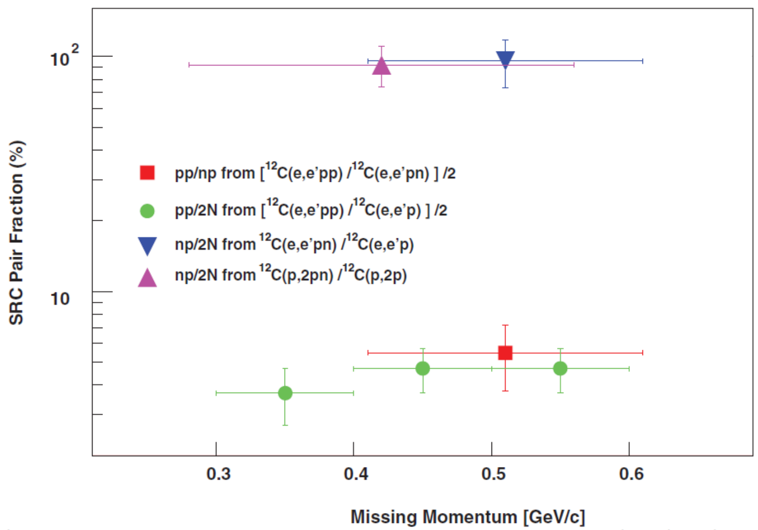

Fig. 2. The fractions of correlated pair combinations in carbon as obtained from the (e,e'pp) and (e,e'pn) reactions, as well as from previous (p,2pn) data. The results and references are listed in table S1.

A. Malki *et al*., PRC65,015207(2002)
A. Tang *et al*., PRL90, 042301(2003)
E. Piasetzky et al., PRL 97, 162504(2006)
^{12}C(p,ppn) at BNL, Beam: 5.9-9.0 GeV/c

(e,e'pp)とは相関があるcosγの領域がずいぶん異なるが...
分解能のせい？

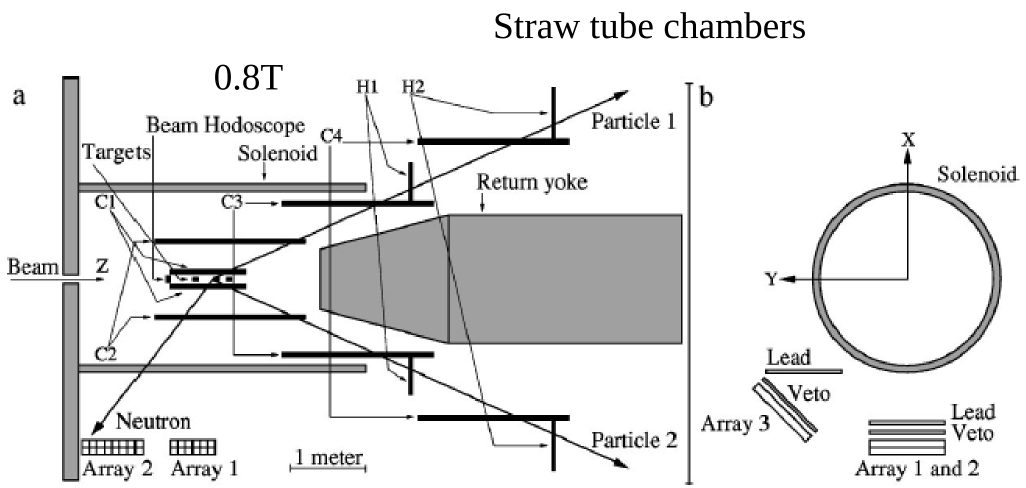

FIG. 4. A schematic side view (a) and a head-on view (b) of the EVA spectrometer and the neutron counter arrays.

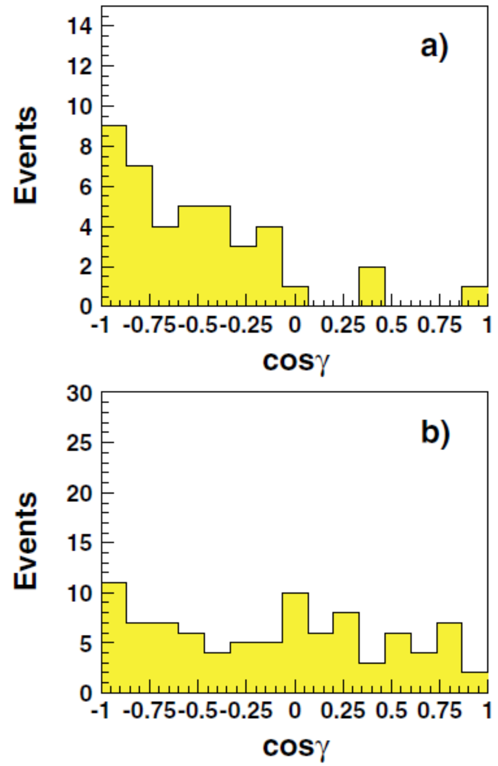

FIG. 2 (color online). Plots of $\cos\gamma$, where γ is the angle between $\mathbf{p}_n$ and $\mathbf{p}_f$, for $^{12}\mathrm{C}(p, 2p + n)$ events. Panel (a) is for events with $p_n > 0.22$ GeV$/c$, and panel (b) is for events with $p_n < 0.22$ GeV$/c$; 0.22 GeV$/c = k_F$, the Fermi momentum for ^{12}C.

$$\frac{^{12}\mathrm{C}(p,ppn)}{^{12}\mathrm{C}(p,pp)} = 92 + 8 - 18\%$$

for p-momentum of 275-500 MeV/c

Results: Ratio between a *p-n* pair and a *p-p* pair

$$\frac{^{12}\mathrm{C}(e,e'pn)}{^{12}\mathrm{C}(e,e'pp)} = 8.1 \pm 2.2$$

Final State Interaction の効果 (distortion, re-scattering)

↓

Attenuation はpとnでキャンセルすると仮定。

Single-Charge Exchange が主に効く

↓

FSIがnがpに変化する寄与。Glauber近似計算で 11%の寄与

$$\rightarrow 9.0 \pm 2.5$$

p-p pair は、*p-n* pair に比べて観測される場合の数が2倍大きい。

$$\rightarrow 18 \pm 5$$

p-n pair の存在確率は、*p-p* pair に比べて18倍大きい

R. Schiavilla et al., PRL98, 132501(2007)

Variational Monte-Carlo Calc.
AV18 and Urbana-IX

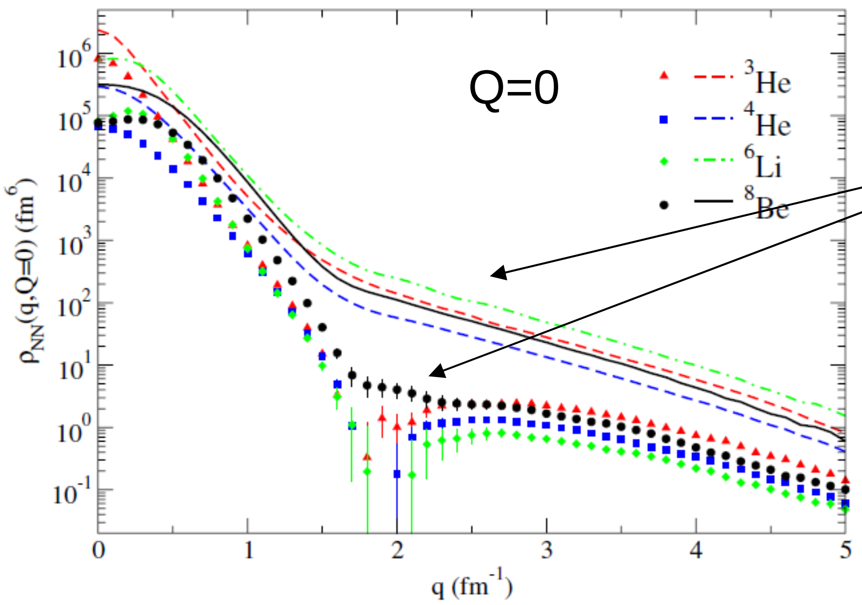

FIG. 1 (color online). The *np* (lines) and *pp* (symbols) momentum distributions in various nuclei as functions of the relative momentum *q* at vanishing total pair momentum *Q*.

*pn*ペア (曲線)の密度は、*pp*ペア(記号)の密度よりもずっと大きい

"the *np* cross section should be at least an order of magnitude larger than the *pp* for relative momenta within (300-600) MeV/c"

q=0　付近では、*np*と*pp*の比は、それぞれのペアの組み合わせ数に近づいている。

“The dominance of the p-n over p-p SRC pairs is a clear consequence of the nucleon nucleon tensor force.”

“It is robust and does not depend on exact parameterization of the nucleon-nucleon force, type of the nucleus, or the exact ground-state wave function used to describe the nucleons”

n-pのcorrelationは非常に大きいので、少量の陽子が混じっているだけでも、中性子星の構造に大きな影響を与えるかも。
Neutrino cooling など。

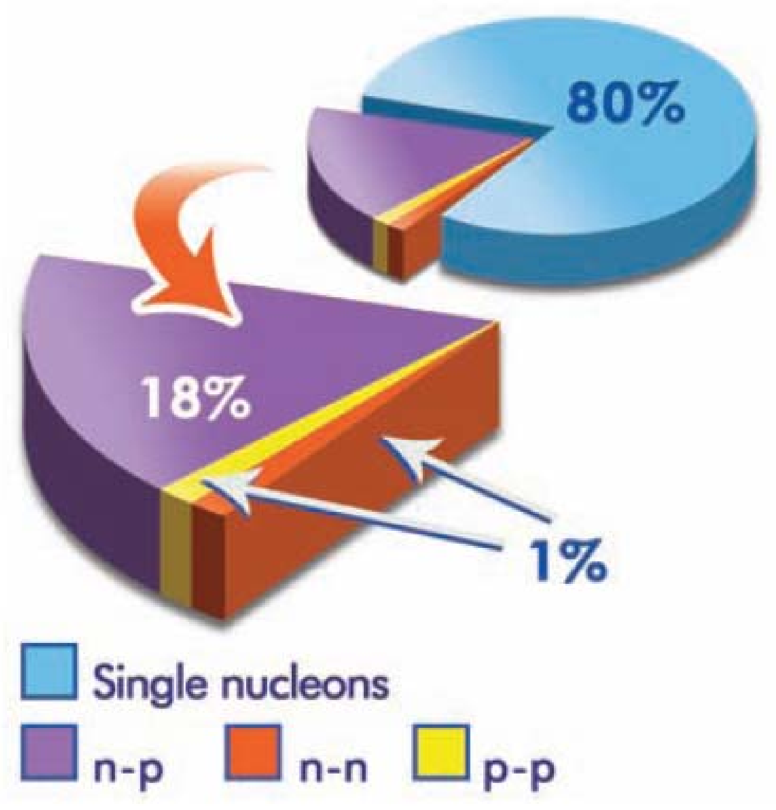

Fig. 3. The average fraction of nucleons in the various initial-state configurations of ^{12}C.

Remarks on E314

- E314と(e,e’*pN*)は同じ物理を見ているのか？ ... おそらくYes。

  E314では^{12}Cと^{16}Oの差に着目しているところが異なる(面白い)。
  n-n相関が直接測定可能(n-を検出すれば)

- knock-outされる核子の核内orbitとrecoilで出てくる核内核子のorbitを特定し、相関のorbitへの依存性を見ることができるはず。

- recoil側の*p*と*n*のdetection方法が大きく異なるため、比を論じる時に問題を生じないか？

  ピックアップ側を変えて、(d,^{3}Hep)と(d,tp)を比較しては？

- (p,d)は表面付近のnをピックアップしやすい？ それでも良い？

- $(\vec{p},d\vec{p})$の偏極移行を測れれば、*p*-*n*ペアがスピン1に組んでいたという情報が引き出せる？もちろん終状態の2粒子のスピン相関を測ればその方が良いが。

Appendix

W.H. Dickhoff and C. Barbieri, Prog. in Part. and Nucl. Phys. 52, 377 (2004)

Long Range Correlation: 2nd-order self energy

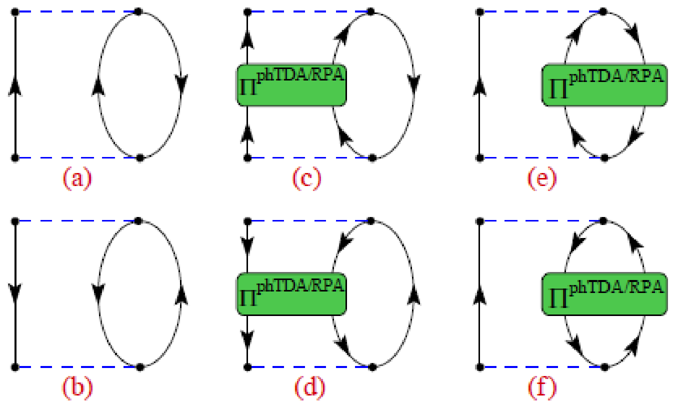

Fig. 37. Second-order self-energy terms represented by Goldstone diagrams (a) and (b). Extensions are made by including TDA or RPA correlations in the particle–particle (diagrams (c) and (d)) or particle–hole channel (diagrams (e) and (f)).

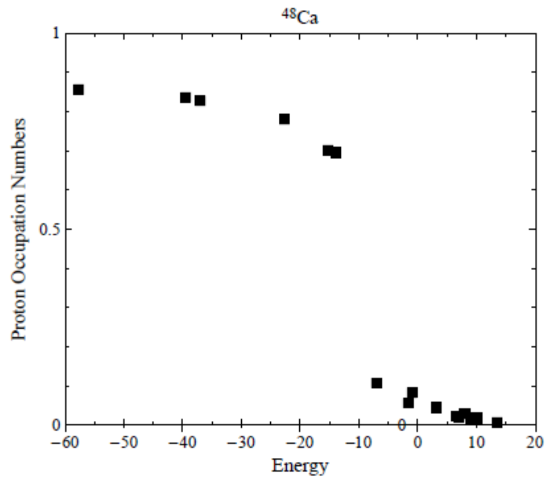

Fig. 39. Proton shell occupation probabilities deduced from a comparison of the present calculation and the (e, e′p) data [201]. The figure displays the calculated values with the ppTDA correlations in the self-energy, multiplied by a factor 0.9 to simulate the effect of short-range correlations.

SRC を simulate するため、0.9のfactorが掛かっている。